PHYSICAL REVIEW B **66**, 161409(R) (2002)

From atomic kinks to mesoscopic surface patterns: Ionic layers on vicinal metal surfaces

S. Fölsch,[1,2,*] A. Riemann,[1] J. Repp,[1,3] G. Meyer,[1,3] and K. H. Rieder[1]
[1]*Institut für Experimentalphysik, Freie Universität Berlin, D-14195 Berlin, Germany*
[2]*Paul-Drude-Institut für Festkörperelektronik, D-10117 Berlin, Germany*
[3]*IBM Research Division, Zurich Research Laboratory, CH-8803 Rüschlikon, Switzerland*
(Received 23 August 2002; published 30 October 2002)

A highly regular assembly of three-sided pyramids can be fabricated by growing the ionic insulator NaCl on the kinked metal surface Cu(532). Only two pyramid faces are covered by NaCl, resulting in an overall surface structure which is modulated in surface chemical behavior. Scanning tunneling microscopy shows that the underlying restructuring mechanism can be attributed to a clear-cut criterion for enhanced interface stability mediated by electrostatic interactions. This criterion provides a generally applicable guideline to create nano- to mesoscopic surface structures by design.

DOI: 10.1103/PhysRevB.66.161409 PACS number(s): 68.35.−p, 68.65.−k, 68.37.Ef, 81.07.−b

Various applications in modern solid-state electronics are based on composite materials in which constituents with different physical properties are combined to create new functions. Examples include metallic and semiconductor superlattices used as magnetic sensors[1] or solid-state lasers.[2] Device performance generally relies on structural control while fabricating such structures by molecular-beam epitaxy (MBE). Ideally, the formation of sharp and lattice-matched interfaces is desirable which in reality is often hampered by the specific bonding behaviors and atomic geometries involved. In addition to the fabrication of artificial superlattices, the lateral structuring of materials at a substrate surface enables to create structures of even lower dimensionality which exhibit new magnetic and electronic behavior. Lateral structuring can be achieved by growth-mediated processes due to, e.g., strain relief[3] or by selective growth at steps,[4] dislocations,[5] or facets.[6] In this case, the ultimate goal is to control the shape, the size and the regularity of the structures produced. Our present study shows that the atomic interfacial structure between two materials of fundamentally different character, namely a wide-band gap insulator and a metal, is determined by very general rules which lead to the formation of highly stable and sharp interfaces. We reported recently[7] that an exceptionally high interface stability arises when the alkali halide (AH) NaCl, a chemically inert ionic insulator, is grown on the stepped copper surface Cu(311). The stabilization is due to an enhanced and localized binding by means of electrostatic interactions between the ions of the (100)-oriented AH film[8] and the dipoles associated with the steps of the metal surface (the step dipoles arise from the Smoluchowski smoothing effect of the electron charge[9]). Here, it is demonstrated that this stability criterion is of general applicability to corrugated metal surfaces of suitable geometry. Depending on the orientation of the metal host, this circumstance can be exploited either to grow ultrathin insulator films of high perfection or to create nano-sized surface patterns by design.

As an exemplary case, we discuss the MBE growth of NaCl (Ref. 10) on the kinked surface Cu(532) studied by low-temperature scanning tunneling microscopy at (STM) 6 K. The bulk-terminated surface structure corresponding to Cu(532) orientation can be obtained by standard preparation procedures under ultrahigh vacuum.[11] In the present case, repeated Ne^+ sputtering and subsequent annealing at $\sim$750 K were applied. The Cu(532) surface geometry is illustrated by the sphere model in Fig. 1(a) where 8 atomic layers are shown (the kink atoms in the topmost layer are indicated in light blue). It is instructive to describe the Cu(532) surface as a kinked Cu(211) surface; the latter is a stepped surface composed of (111) and (100) microfacets. The red dashed line in Fig. 1(a) denotes a (211)-oriented terrace which measures one step spacing along the $[1\bar{1}\bar{1}]$ direction perpendicular to the steps and two Cu-Cu spacings

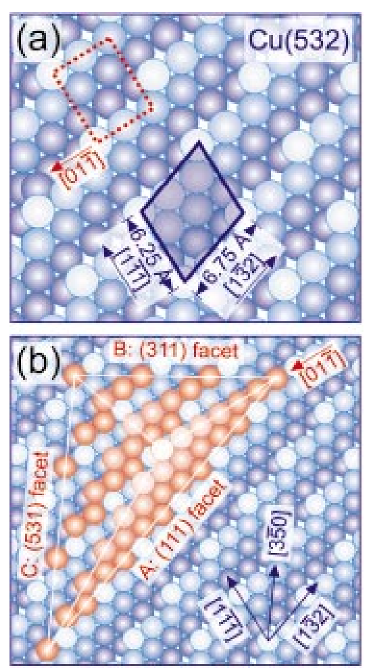

FIG. 1. (Color) (a) Sphere model of Cu(532) showing 8 atomic layers (kink atoms in the topmost layer indicated in light blue) and the oblique unit cell (blue line). The red dashed line indicates a (211)-oriented terrace measuring one step spacing perpendicular to the steps and two Cu-Cu spacings along the $[01\bar{1}]$ step direction. (b) Atomic structure of a pyramid with a (111) facet (A), a (311) facet (B), and a (531) facet (C) built up by incorporating additional Cu atoms (red spheres) along the $[01\bar{1}]$ step direction.

0163-1829/2002/66(16)/161409(4)/$20.00

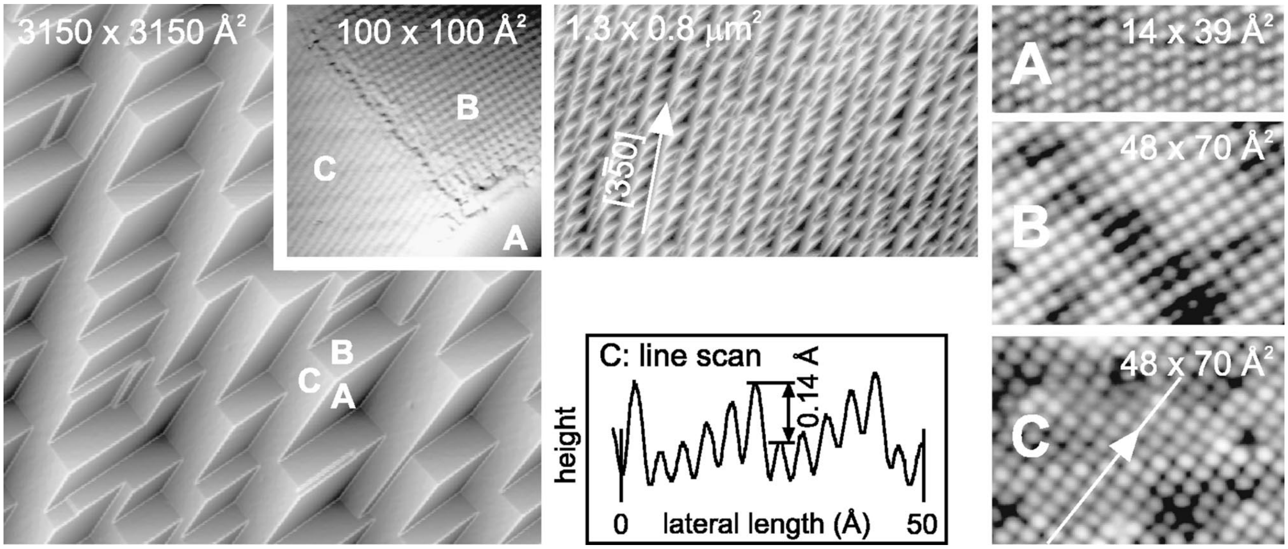

FIG. 2. (left) STM image of the reorganized surface after growing ~0.6 ML at 600 K (3150 Å×3150 Å) showing three well defined facet orientations; the inset (100 Å×100 Å) shows that facets B and C are covered by (100)-terminated NaCl while facet A is still bare Cu. The large-area scan (center, 1.3 μm×0.8 μm) shows that the evolving surface topography is of high regularity on the mesoscopic scale. (right) Atomically resolved STM images of the Cu(111) facet (A, 14 Å×39 Å), the NaCl-covered (311) facet (B, 48 Å×70 Å), and the NaCl-covered (531) facet (C, 48 Å×70 Å). The line scan (center) was taken along the close-packed Cl rows (as marked in image C) and visualizes the defect step structure of the (531) facet.

along the $[01\bar{1}]$ step edge direction. The Cu(532) surface is then generated by incorporating kinks every two and a half Cu-Cu spacings along the step edges and the resulting surface symmetry is described by an oblique unit cell measuring 6.25 Å along $[1\bar{1}\bar{1}]$ and 6.75 Å along $[1\bar{3}2]$. Upon NaCl deposition at elevated temperature the Cu(532) template reorganizes into a regular assembly of nano-sized pyramids. As a common feature of adsorbate-induced faceting,[12] this restructuring effect indicates an enhanced energetic stability of the facets formed. The STM image on the left of Fig. 2 shows the resulting surface topography after growing ~0.6 monolayers (ML)[13] at 600 K. Three facet types are formed (labeled as A, B, and C) which exhibit well-defined crystallographic orientations. We performed supplementary high-resolution low-energy electron diffraction measurements to determine the corresponding facet orientations and found a (111) orientation for type A, a (311) orientation for type B, and a (531) orientation with a superimposed defect step structure for type C (the latter is discussed in detail below). Figure 1(b) visualizes the atomic structure of these facets and their arrangement relative to the Cu(532) surface. For the sake of clarity the defect steps of the (531) facet are omitted in the scheme. Note also that only Cu atoms are shown; the positioning of the NaCl adlayer will be addressed later. The azimuthal orientation of the sphere model is the same like that of the STM images in Fig. 2. The blue spheres represent atoms of the Cu(532) surface whereas the red spheres denote additional Cu atoms incorporated along the $[01\bar{1}]$ direction. In this way, a pyramid is built up which is terminated by three different facet orientations corresponding to the close-packed (111) plane, the stepped (311) plane, and the kinked (531) plane. The large-area scan in Fig. 2 (center, 1.3 μm ×0.8 μm) shows that the evolving surface topography is of high regularity on the mesoscopic scale: The (111) and (311) facets (A and B) form staircase-like columns aligned with the $[3\bar{5}0]$ direction which are separated by extended (531) facets (C). Along the staircase the mean spacing of equivalent facets measures ~500 Å while the mean separation of adjacent columns perpendicular to the $[3\bar{5}0]$ direction is ~570 Å. These characteristic dimensions sensitively depend on the substrate temperature (i.e., on the Cu adatom mobility) during AH deposition; they are reduced by a factor of 2 when performing the growth at 500 K.

The energetic driving force for the formation of the observed facet orientations and the chemical composition of the resulting surface structure is clarified by STM measurements performed with atomic resolution. The inset on the left of Fig. 2 (100 Å×100 Å) shows a single pyramid imaged at 1 nA and +30 mV corresponding to a tunneling resistance of 30 MΩ (the tunneling voltage refers to the sample with respect to the tip): While the (311) and the (531) facets (B and C) exhibit a marked atomic corrugation, the (111) facet (A) does not. At considerably lower tunneling resistance (i.e., at enhanced tip-sample interaction) an atomic corrugation is observed also for the (111) facet. Such a case is illustrated by the image labeled as A on the right of Fig. 2 (14 Å×39 Å, 0.14 μA, +26 mV) reproducing hexagonal symmetry and a periodicity of ~2.5 Å along the close-packed rows (cf. $a_{Cu}/\sqrt{2}=2.55$ Å, with the Cu lattice constant $a_{Cu}=3.61$ Å). Obviously, the (111)-oriented facets of the reorganized surface correspond to bare Cu(111) facets. In contrast, the image labeled as B (48 Å×70 Å) indicates that the (311)-oriented facet is overgrown by a (100)-terminated NaCl monolayer, in analogy to our previous findings for the growth system NaCl/Cu(311)[7] (note that STM images only the Cl ions as protrusions[14]): In the case of Cu(311), the

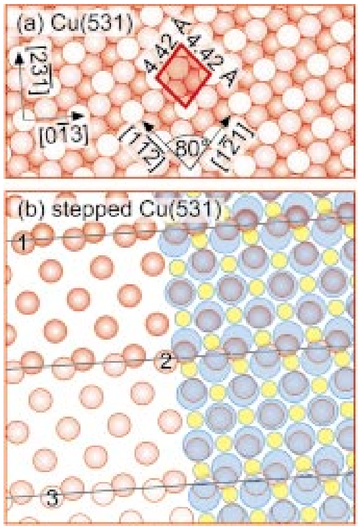

FIG. 3. (Color) (a) Sphere model of bare Cu(531) obeying rhombic symmetry with a kink spacing of 4.42 Å and an angle of 80° between $[1\bar{1}2]$ and $[1\bar{2}1]$. (b) Structure model with four Cu(531) terraces (only kink atoms are shown, cf. red spheres) separated by defect steps (cf. black lines) that are 14.40 Å apart and run along $[0\bar{1}3]$. The stepped Cu(531) template coherently matches with a virtually strain-free NaCl(100) monolayer (right) with the Cl ions (blue) located close to the kink atom positions and the Na ions (yellow) in between.

intrinsic Cu steps run along the $[01\bar{1}]$ direction [cf. sphere model in Fig. 1(b)] with a step spacing of 4.23 Å. This value is close to the intrinsic Cl-Cl spacing of NaCl ($a_{\mathrm{NaCl}}/\sqrt{2}=3.99$ Å in the bulk). As a consequence, the ionic layer is pinned by the step dipoles via electrostatic interactions with the Cl rows located on top of the Cu step edges.[7] This leads to a cubic arrangement of the Cl positions in image B with the polar $\langle 110\rangle$ directions oriented parallel and perpendicular to the Cu steps. Next, we verify that also the (531)-oriented facet is stabilized by electrostatic interactions between the ionic charges of a (100)-terminated NaCl monolayer and the charge modulation of the Cu template. The sphere model in Fig. 3(a) shows that the kink positions of bare Cu(531) obey rhombic symmetry with a separation of 4.42 Å and an angle of 80° between the $[1\bar{1}2]$ and the $[1\bar{2}1]$ direction. It is the kink atoms which are expected to carry a positive charge due to the Smoluchowski smoothing effect. The related STM image C in Fig. 2 indeed shows an atomic corrugation with square structure and a lattice constant of ~ 4 Å which thus resembles the kink arrangement of bare Cu(531). Crucially, monatomic Cu defect steps are formed at the NaCl/Cu(531) interface which, as will be shown below, allow for effective strain relaxation in the overlayer. These steps run along the $[0\bar{1}3]$ direction [indicated in Fig. 3(a)] with a mean separation of ~ 14 Å and give rise to an undulation of the NaCl overlayer; the undulation is evident from the faint gray scale modulation onto facet C in the (100 Å×100 Å)-sized inset in Fig. 2. The height variation of the undulation measures ~ 0.14 Å which is considerably smaller than the monatomic defect step height of Cu(531) [$a_{Cu}/\sqrt{35}=0.61$ Å]. This suggests a carpetlike growth mode as it is commonly observed for ultrathin AH films on surfaces with defect steps.[14,15] By measuring the corrugation along the close-packed Cl rows as indicated in image C (the Cl rows are inclined by $\sim 45°$ relative to the step edges) we find that the underlying Cu steps are crossed every five Cl-Cl spacings (cf. line scan in Fig. 2). This observation is readily explained by the structure model in Fig. 3(b) which shows four Cu(531) terraces (only the kink atoms are drawn, cf. red spheres) separated by defect steps (cf. black lines) that are 14.40 Å apart and run along the $[0\bar{1}3]$ direction. In accordance with the line scan in Fig. 2 the steps in Fig. 3(b) correspond to downward steps when moving from the bottom to the top. The essential effect of a defect step is that kink atom positions of adjacent (531) terraces are shifted not only vertically but also laterally. Figure 3(b) shows that this circumstance enables a coincident matching between the stepped Cu(531) template and a virtually strain-free NaCl(100) monolayer with the Cl ions (cf. blue spheres) located close to the kink atom positions. According to the structure model, the Cl-Cl spacing along the direction close to $[1\bar{1}2]$ is 4.15 Å (equal to 1/5 of the distance between the kink atoms labeled as 1 and 2) while that along the direction close to $[1\bar{2}1]$ measures 3.99 Å (1/5 of the distance between the kink atoms 2 and 3) with an angle of 89.1° between the two directions (cf. $a_{\mathrm{NaCl}}/\sqrt{2}=3.99$ Å and 90° for bulk NaCl). The precise layer structure certainly involves also minor relaxations of the atomic positions. Nonetheless, our simplified model based on a nearly bulk-like (1×1) layer is capable to identify the energetic constraint that drives the formation of the apparently complex Cu facet orientation observed: The attempt is to achieve an optimized matching between the charge modulation of the metal template and the lateral ion positions while keeping the AH overlayer in a state of low strain.

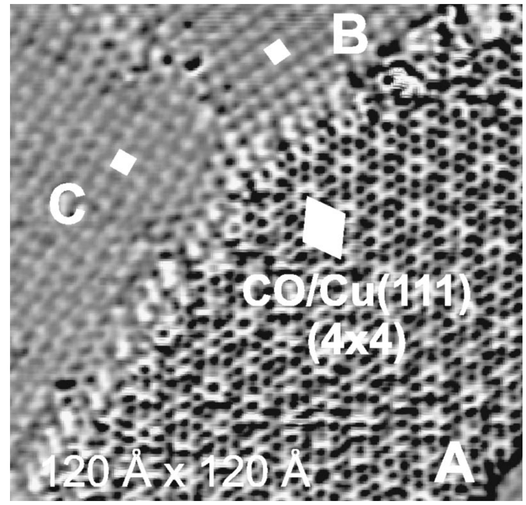

FIG. 4. STM image (120 Å×120 Å) of a single pyramid after exposure to 10 L CO at 85 K demonstrating the chemical selectivity of the reorganized surface. Facets B and C still exhibit an atomic corrugation with square symmetry [according to NaCl(100)] while the bare Cu(111) facet (A) exhibits a characteristic (4×4) superstructure indicative for the CO/Cu(111) saturation phase.

Finally, we verify the chemical selectivity of the fabricated surface pattern. The STM topograph in Fig. 4 (120 Å

$\times 120$ Å, 240 pA, -38 mV) shows a single pyramid after exposure to 10 Langmuir CO at 85 K. The image has been filtered in order to simultaneously display all three facet types at the same gray scale. As evident, the facets B and C still exhibit an atomic corrugation with cubic symmetry which corroborates that these facets are passivated by the chemically inert NaCl(100) termination. In contrast, CO adsorption takes place onto the bare Cu(111) facet (A) and leads to the formation of a characteristic (4×4) superstructure which is indicative for the CO saturation phase on Cu(111) as observed previously by STM under comparable dosing conditions.[16] The AH-mediated faceting process thus provides a nanoscopic masking procedure which allows to engineer spatial modulations in surface chemical behavior.

In conclusion, the crucial role of electrostatics for the binding between an ionic insulator and a stepped or kinked metal template[17] provides a simple criterion to predict interfacial geometries of enhanced stability. Those interfaces are highly stable for which the charge modulation of the metal substrate matches with the ionic charges of the overlayer. This energetic preference can be exploited to engineer nanoscale surface patterns if (i) the ionic deposit provides a pronounced directional anisotropy in the surface free energy [as it is the case for alkali halides[8]], (ii) a facet orientation fulfilling the stability criterion is available close to the macroscopic substrate surface orientation, and (iii) sufficient substrate adatom mobility allows for the required mass transport. The shape of the pattern can be controlled by the symmetry of the starting surface: While stripelike facet structures are formed on stepped substrates [as we reported previously for Cu(211)],[18] the exemplary case presented here shows that dotlike structures (i.e., nano-sized pyramids) can be produced on kinked substrates. Since the deposit grows selectively on the corrugated metal facets one obtains a nanoscopic masking effect of the surface. Hence, this class of insulator-on-metal systems is of prerequisite relevance for the lateral structuring of subsequently deposited material by selective decoration since it includes all essential requirements, namely a means to control the shape and the size of the fabricated structures combined with a spatial modulation in surface chemical behavior.

This research was supported by the Volkswagen-Stiftung (I/72 417) and the Deutsche Forschungsgemeinschaft (RI 472/3-2, Sfb 290/TPA5).

*Email address: foelsch@pdi-berlin.de

[1] C.H. Tsang *et al.*, IBM J. Res. Dev. **42**, 103 (1998).

[2] Y. Arakawa and A. Yariv, IEEE J. Quantum Electron. **22**, 1887 (1986).

[3] J. Tersoff and R.M. Tromp, Phys. Rev. Lett. **70**, 2782 (1993).

[4] M. Mundschau, E. Bauer, and W. Swiech, J. Appl. Phys. **65**, 581 (1989).

[5] H. Brune, M. Giovannini, K. Bromann, and K. Kern, Nature (London) **394**, 451 (1998).

[6] R. Nötzel *et al.*, Phys. Rev. Lett. **67**, 3812 (1991); C. Teichert *et al.*, Appl. Phys. Lett. **74**, 588 (1999).

[7] J. Repp, S. Fölsch, G. Meyer, and K.H. Rieder, Phys. Rev. Lett. **86**, 252 (2001).

[8] The surface free energy of AH bulk crystals is strongly minimized for the (100) termination [cf. A.C. Shi and M. Wortis, Phys. Rev. B **37**, 7793 (1988), and references therein].

[9] R. Smoluchowski, Phys. Rev. **60**, 661 (1941).

[10] NaCl was evaporated from a Al_2O_3 crucible at ~ 1000 K; under these conditions sublimation takes place in molecular form [cf. G.M. Rothberg, M. Eisenstadt, and P. Kusch, J. Chem. Phys. **30**, 517 (1959)].

[11] G. Witte *et al.*, Phys. Rev. B **58**, 13 224 (1998).

[12] See, e.g., T.E. Madey *et al.*, Surf. Sci. **438**, 191 (1999); M. Horn-von Hoegen, A. AlFalou, B.H. Müller, U. Köhler, L. Andersohn, B. Dahlheimer, M. Henzler, Phys. Rev. B **49**, 2637 (1994).

[13] 1 ML refers to the density per area of (100)-terminated NaCl (6.3×10^{18} cm^{-2}).

[14] W. Hebenstreit *et al.*, Surf. Sci. **424**, L321 (1999).

[15] C. Schwennicke, J. Schimmelpfennig, and H. Pfnür, Surf. Sci. **293**, 57 (1993).

[16] L. Bartels, G. Meyer, and K.H. Rieder, Surf. Sci. **432**, L621 (1999).

[17] M. Stoneham, Nature (London) **410**, 159 (2001).

[18] S. Fölsch *et al.*, Phys. Rev. Lett. **84**, 123 (2000).